JOURNAL OF MATERIALS SCIENCE 17 (1982) 821–831

Surface contours in the axi-symmetric upsetting of solid cylinders

A. P. SINGH*, K. A. PADMANABHAN
Department of Metallurgy, Indian Institute of Technology, Madras-600036, India

Surface flow contours during the axi-symmetric upsetting of aluminium, Sn–Pb eutectic alloy and Plasticine have been studied as a function of the extent of deformation, frictional condition and height-to-diameter ratio. The roughness of the end faces after upsetting has also been measured. The results have been explained in terms of the changes in the frictional condition, the strain-rate sensitivity and the local strain rate and it is concluded (a) that cold upsetting of a material of negligible strain-rate sensitivity gives rise to a parabolically-shaped barrel, (b) that hot upsetting the Sn–Pb alloy specimens of height-to-diameter ratio 1.5 results in a linear increase in diameter from the top to the bottom of specimens, due to a linear decrease in strain rate in the same direction, (c) that hot compression of Plasticine specimens and Sn–Pb alloy specimens of height-to-diameter ratio 2.0 leads to complex shape changes which cannot be predicted using the present knowledge concerning the upsetting of strain-rate sensitive materials and (d) that the greater increase in roughness following significant compression of the end faces of lubricated specimens, compared with that observed for unlubricated specimens, is due to enhanced surface metal flow with a decrease in frictional constraints.

1. Introduction

The type of metal flow in a given operation determines the final shape of the product, the defects present and the variations in properties due to localization of flow. The extent of localization of flow, on the other hand, is affected by grain size and distribution, preferred orientation, imposed strain rate, temperature of deformation, effectiveness of lubrication and tool geometry [1].

Experiments to study the flow of metals involve the use of the actual metals and alloys or model materials, e.g., Plasticine. The distortion of grid lines or the differential etching of a section of the deformed specimen has been used to assess strain distribution. A systematic study of the change in geometry of the free surfaces can be used also in predicting metal flow under different conditions of working. This is because the boundaries in contact with tool surfaces will have to conform to the tool geometry. The changes in the geometry of free surface(s) define the overall deformation.

Thus, a study of free deformation can simplify the design of forgings and decrease the number of trials necessary before successful forgings can be made.

Usually secondary tensile forces (which cause cracking) develop only at the free surfaces. This would imply that, if the extent of barrelling can be predicted, then the limits to formability under the given working condition can be fixed.

Alexander and Brewer [2] have explained how non-uniform distortions can result, even where they are not expected, if a specimen with the wrong geometry is chosen. Johnson and Mellor [3], on the other hand, have discussed in detail the effect of specimen geometry and flow characteristics of materials on the shape changes accompanying free deformation. During explosive working of metals [4] pressure waves, work-piece geometry and material response are all known to influence the resulting changes in shape.

In general, the change in the shape of the work-piece following a particular tool movement cannot

*Present address: Research and Development Centre for Iron and Steel, Steel Authority of India Ltd, Ranchi-2, India.

0022–2461/82/030821–11$03.82/0

be easily predicted. Indeed there is a suggestion [5] that for free flow the change in contour has not been predicted for even a single practical problem. The upsetting of cylinders, however, has received some attention [6]. Here, both the height-to-diameter ratio and the frictional condition are important in determining the shape of the barrel.

In hot upsetting the insulating properties of the lubricant may greatly affect the metal flow. In one case [7] the strain distribution was more uniform at higher speeds of deformation while in another [8] non-uniformity in flow increased with increasing strain and strain rate. Occasionally, concave bulging ("bollarding") has also been reported [9].

Frequently, an appropriate choice of lubricant, die finish and operating conditions ensures a lustrous finished product. Use of a light lubricant results in highly reflective surfaces but a viscous lubricant causes a matt finish. Surface roughness of the work-piece also affects the effectiveness of lubricants [10–21].

In view of the above, it is very desirable to be able to predict accurately the flow profiles that develop during upsetting. An examination of the literature (see, for example, [22]), however, reveals that even with simplifying assumptions the analytical approach is rather complicated. Therefore, an attempt has been made in this paper to develop empirical curvilinear regressional equations for predicting the surface contours obtained in axi-symmetric upsetting. Also, the roughness of the flat, compressed faces, under different experimental conditions, has been characterized, both in terms of the arithmetical mean roughness value and the pure depth value.

2. Experimental procedure

Commercial aluminium, tin–lead eutectic alloy (62 wt% Sn–38 wt% Pb) and black Plasticine were chosen for the present study.

Commercial aluminium, having the composition 0.18 wt % Fe–0.12 wt % Si–99.7 wt % Al, was received in the form of an ingot. It was remelted in a crucible furnace and cast into cylindrical bars of 25.4 mm diameter. These bars were cold forged at room temperature to a diameter of 12.70 mm. Cylindrical specimens having a constant diameter of 10.16 mm and a height-to-diameter ratio of 1.5 were machined from the forged rods. The specimens were annealed at 673 K for 1 h. The grain size after annealing was 73 μm.

The tin–lead eutectic alloy was melted in a resistance furnace and cast into bars of 25.4 mm diameter. These bars were forged at room temperature, i.e., hot-worked, to a diameter of 12.70 mm. Cylindrical specimens of dimensions identical to the previous case were made and annealed at 373 K for 15 min. A grain size of 6.2 μm was obtained.

Plasticine specimens, with dimensions similar to the other two cases, were made using a split die.

Some Sn–Pb alloy specimens with a diameter of 10.16 mm and a height-to-diameter ratio of 2.0 were also made.

The specimens were compressed axially on an Instron universal testing machine at a constant cross-head speed of 1.67 mm ksec^{-1} by amounts varying between 10 and 50 per cent reduction in height. The tests were carried out in both the dry and lubricated conditions. For commercial aluminium and Sn–Pb eutectic alloy specimens thin general-purpose lithium-base grease was chosen as the lubricant; in the case of Plasticine "Tee-pol" solution was used.

The profile developed on the curved surface of the aluminium and the Sn–Pb cylinders was plotted with the aid of a profile projector at a suitable magnification (x 20). With Plasticine, because of its ultra-softness, photographic negatives were projected, at a magnification of 50, to determine the profiles.

In addition, using a Perth-o-meter the roughness of the flat, compressed, faces of the aluminium and the Sn–Pb alloy specimens was evaluated in terms of both the arithmetical mean roughness value, R_a, and the pure depth value, R_t. (In a Perth-o-meter the oscillations resulting from the movement of a diamond stylus over the given surface is recorded on a strip chart, after suitable magnification.) R_a is determined by averaging both the peaks and the valleys to two mean profile lines, so that the distance between these two lines gives the mean roughness value. R_t is the vertical distance between the highest peak and the lowest valley in the entire length of traverse.

The experiments on commercial aluminium simulated conditions of cold work, while those involving the Sn–Pb alloy and Plasticine correspond to the hot working situation. The strain rate employed, however, was slower than the industrial level by a factor of about 1000. (The commercial implications of the results obtained under these conditions will be discussed in Section 4.)

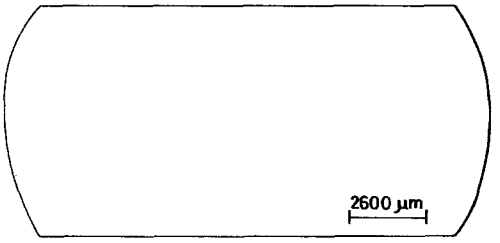

Figure 1 Barelling in commercial aluminium compressed by 50%.

3. Results

Following the procedure outlined earlier, the curved surfaces of the various deformed samples were traced. A polynomial prediction equation was obtained for each specimen using the method of least-squares fit. By comparing the equations for the contours on either side of the axis of symmetry, it could be established that within experimental errors flow was symmetric about the axis of the cylinder.

For the commercial aluminium specimens the surface contour in the entire range of 10 to 50% reduction (defined as $(H_0 - H_f)/H_0$, where H_0 is the initial height and H_f is the height following deformation) could be represented by a parabola (see, for example, Fig. 1). The form of the equation predicting the surface shape was little affected by friction at the interface, although barrelling decreased by about 5% when a lubricant was used. The prediction equations corresponding to five different reductions are presented in Table I. In Table I the standard deviation and the coefficient of variation associated with each prediction equation, the true stress at the bottom of stroke for each compression and the percentage decrease in barrelling, defined in terms of the maximum diameter, are also given.

For tin–lead eutectic alloy specimens having a height-to-diameter ratio of 1.5 the profile was linear with the specimen diameter increasing from the top, i.e., the surface in contact with the moving anvil, to the bottom, e.g., Fig. 2. Lubrication did not alter the surface contour. The flow stress also did not change. The prediction equations and the other details are summarized in Table II.

The profiles obtained by deforming Plasticine were distinctly different from those seen with other materials, see Fig. 3 a to e. Here again the use of a lubricant did not change the profile, extent of barrelling or the flow stress.

If the entire profile was fitted to a single equation by taking the origin to lie at the uppermost point, it was necessary to use a third or fourth degree curve (see Table IIIA and B, respectively). Closer examination, however, revealed that the compound curve in each case could be described in terms of simpler configurations. Except when the degree of compression was 20%, it was found that up to a distance $H_f/2$ from the top the profile was linear with an outward slope. The rest of the curve could be represented by a parabola. When the degree of compression was 20%, the linear portion was absent. The compound curve in this case could be represented by two parabolas, the first curve terminating at a distance $H_f/3$ from the

TABLE I Prediction equations for commercial aluminium compressed, with and without a lubricant, by different amounts

$\left(\frac{H_0 - H_f}{H_0}\right) \times 100$ (%)	Prediction equation* (measurement in cm)	Standard deviation (± cm)	Coefficient of variation (%)	True stress at the end of stroke† ($MN\,m^{-2}$)	Decrease in extent of bulging when a lubricant was used (No lubrication condition is base) (%)
10	$y = 0.90 + 0.0052x - 0.0058x^2$	0.028	0.6	66 62	5.6
20	$y = 1.3034 + 0.0061x - 0.0104x^2$	0.017	0.2	82 78	5.5
30	$y = 1.86 + 0.0084x - 0.0198x^2$	0.018	0.1	93 89	5.4
40	$y = 1.90 + 0.0112x - 0.0112x^2$	0.011	0.1	101 96	5.3
50	$y = 2.00 + 0.0158x - 0.0357x^2$	0.032	0.3	107 102	4.8

*The origin has been assumed to lie along a horizontal line at $H_f/2$ from the top surface of the specimen. (The dimensions of the compression specimen have been magnified 20 times to obtain the prediction equations.)
†The lower true stress in each compression corresponds to the lubricated condition.

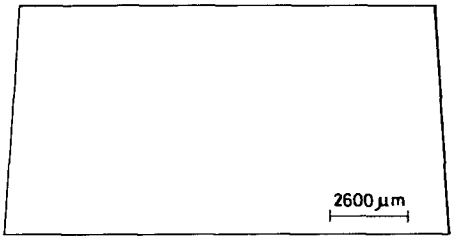

Figure 2 Surface profile in Sn–Pb eutectic alloy of H_0/D_0 ratio 1.5 compressed by 50%.

top. These simplified prediction equations are given in Table IV.

The earlier conclusion [3] that the surface contour depended also on the height-to-diameter ratio received support from the experiments on Sn–Pb specimens having a height-to-diameter ratio of 2.0. In this case two specimens were compressed, without lubrication, by 20% and 30%, respectively. The profiles developed were quite different compared to when the height-to-diameter ratio was 1.5 but were very similar to those obtained with Plasticine, see Fig. 4.

In view of this striking similarity, further experiments were considered unnecessary. In Table VA and B the third and fourth degree equations developed to fit the profiles are presented. The compound curves for this alloy could also be considered to be made up of simpler configurations. The simpler equations obtained by this approach are given in Table VC.

The roughness of the compressed faces, obtained with and without lubrication, was evaluated in terms of both the average, R_a, and the maximum, R_t, values. For each specimen, by evaluating the roughness at both ends, it was ensured that within experimental errors they had similar roughness. Table VI contains the results for aluminium specimens; the results for Sn–Pb alloy specimens, with height-to-diameter ratio of 1.5, are given in Table VII. In both materials, following relatively small deformation, the roughness of the lubricated specimens was less or equal to that of unlubricated specimens. After heavy compression, however, the opposite was true, see Figs 5 and 6 for results concerning commercial aluminium and Sn–Pb eutectic alloy, respectively. No measurements were made of surface roughness for Plasticine since it was too soft.

In order to understand the results presented in the previous paragraph, tracings of the compressed faces corresponding to Figs 5 and 6 were made (Fig. 7: commercial aluminium; Fig. 8: the Sn–Pb alloy). In all specimens an inner circle could be seen, which corresponded to the portion in contact with the platen at the beginning of deformation. It will be seen from Figs 7 and 8 that, after large deformation, the area in contact with the anvil is greater for the lubricated specimens than for the unlubricated specimens.

4. Discussion

Earlier work [19] has revealed that under conditions of cold working "dead metal" cones with an apex angle of approximately 120° are created at either end of the compression specimen. During deformation these zones force the remaining metal transversely outward and cause barrelling. Then, the lateral velocity of flow increases from zero at the metal–tool interfaces to a maximum value at the centre. When this velocity variation is uniform and gradual, the simplest profile is a parabola (as two straight lines will meet along the centre plane with a sharp discontinuity) so long as the height-

TABLE II Prediction equations for Sn–Pb eutectic alloy compressed, with and without a lubricant, by different amounts. Height-to-diameter ratio is 1.5

$\left(\frac{H_0 - H_f}{H_0}\right) \times 100$ (%)	Prediction equation* (measurements in cm)	Standard deviation (± cm)	Coefficient of variation (%)	True stress at the end of stroke† ($MN\,m^{-2}$)
10	No visible deviation from cylindrical shape	–	–	9
20	$y = 0.05655 + 0.03261x$	0.015	0.1	8
30	$y = 0.07501 + 0.0320x$	0.005	0.1	8
40	$y = 0.09076 + 0.03926x$	0.002	0.3	8
50	$y = 0.1050 + 0.05763x$	0.002	0.11	8

*The origin has been assumed to lie on the top surface of the specimen. (The original dimensions of the compression specimen have been magnified 10 times to obtain the prediction equations.)
†The decrease in true stress and extent of barrelling on using a lubricant is negligible.

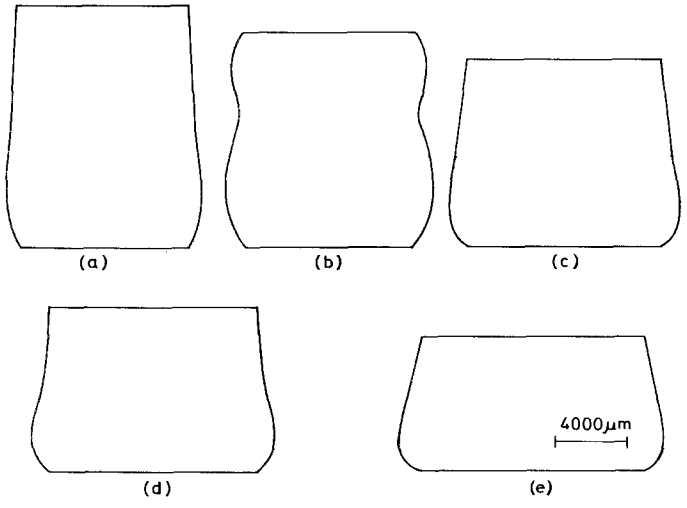

Figure 3 Surface contour in Sn–Pb eutectic alloy of H_0/D_0 ratio 2.0 compressed by 30%.

to-diameter ratio is less than about 2.5 [23]. This is what has been seen in the case of the aluminium specimens (see Fig. 1 and Table I).

For aluminium in the presence of lubrication, barrelling and flow stress decreased by about 5% compared with the unlubricated condition. The difference in the extent of barrelling and flow stress betweeen the lubricated and dry conditions in other materials was negligible. On account of the low strain-rate employed, it is understandable that the frictional contribution is, in general, rather low. In the case of aluminium the use of a

TABLE IIIA Prediction equations for Plasticine compressed, with and without a lubricant, by different amounts for a polynomial fit of degree three

$\left(\frac{H_0 - H_f}{H_0}\right) \times 100$ (%)	Prediction equation* (Measurements in mm)	Standard deviation (± mm)	Coefficient of variation (%)	True stress at the end of stroke† (N cm^{-2})
10	$y = -0.2611 + 1.141x + 0.1937x^2 - 0.3679x^3$	0.05	1.2	6
20	$y = 0.73 - 0.3736x + 0.0586x^2 - 0.0026x^3$	0.06	2.3	7
30	$y = -0.1362 + 0.1289x + 0.082x^2 - 0.00107x^3$	0.01	1.7	7
40	$y = 0.0406 + 0.0439x - 0.0993x^2 + 0.1138x^3$	0.01	2.0	7
50	$y = 0.601 + 0.052x - 0.83x^2 + 0.1235x^3$	0.02	2.4	7

TABLE IIIB Prediction equations for Plasticine compressed, with and without lubricant, by different amounts for a polynomial fit of degree four

$\left(\frac{H_0 - H_f}{H_0}\right) \times 100$ (%)	Prediction equation* (Measurements in mm)	Standard deviation (± mm)	Coefficient of variation (%)	True stress at the end of stroke† (N cm^{-2})
10	$y = 0.1860 - 0.5255x - 0.0127x^2 + 2.8956x^3 - 1.7180x^4$	0.04	0.9	6
20	$y = 0.20 + 0.24x + 0.07x^2 + 0.007x^3 - 0.0001x^4$	0.04	2.6	7
30	$y = 0.1543 - 0.0358x + 0.0058x^2 + 0.0043x^3 - 0.0004x^4$	0.01	1.3	7
40	$y = 0.0106 + 0.11x - 0.607x^2 + 0.1069x^3 - 0.0777x^4$	0.01	1.6	7
50	$y = 0.018 + 0.12x - 0.065x^2 + 0.11x^3 - 0.08x^4$	0.02	2.2	7

*The origin has been assumed to lie on the top surface of the specimen. (The original dimensions of the compression specimen have been magnified 15 times to obtain the prediction equations.)
†The decrease in true stress and extent of barrelling on using a lubricant is negligible.

TABLE IV Prediction equations for Plasticine compressed, with and without a lubricant, by different amounts. (Fit obtained by dividing the compound curves into two parts)

$\left(\frac{H_0 - H_f}{H_0}\right) \times 100$ (%)	Prediction equation* (Measurements in mm)	Standard deviation (± mm)	Coefficient of variation (%)	True stress at the end of stroke† ($N\,cm^{-2}$)
10	$y = 0.0298x - 0.0422$	0.01	0.6	6
	$y = 0.8028x - 0.0989x^2 - 0.8425$	0.01	0.3	
20	$y = 0.3994x - 0.0620x^2 - 0.0538$	0.01	0.7	7
	$y = 0.7348x - 0.0622x^2 - 0.9872$	0.02	0.5	
30	$y = 0.0743x - 0.066$	0.01	0.5	7
	$y = 0.7632x - 0.0215x^2 - 0.3566$	0.01	0.5	
40	$y = 0.1221x - 0.0073$	0.01	0.6	7
	$y = 1.3047x - 0.1513x^2 - 1.8440$	0.01	0.4	
50	$y = 0.10 + 0.20x$	Nil	Nil	7
	$y = 0.8758x - 0.1758x^2 - 0.1985$	0.02	0.6	

*In all cases, except for 20% compression, the ratio of the linear to the quadratic range is 1:1. For 20% compression the first parabola covers a distance $H_f/3$ from the top. (The original dimensions of the compression specimen have been magnified 15 times for obtaining the prediction equations.)
†The decrease in true stress and extent of barrelling on using a lubricant is negligible.

lubricant appears to have slightly decreased the coefficient of friction and the redundant work. Thus, a small decrease in the extent of barrelling and the flow stress is to be expected. For the other materials which are hot worked at room temperature, the effect of lubrication on frictional work appears to be insignificant. Then no change in the extent of barrelling and flow stress is expected.

In the Sn–Pb eutectic alloy specimens of initial height-to-diameter ratio of 1.5, the diameter of the compressed specimens increased linearly from top to bottom. A somewhat similar result has been reported by Padmanabhan [24]. When V is the tool velocity and H is the instantaneous height of the compression specimen, V/H is the strain rate at the top end, in contact with the moving tool, of the specimen. When a linear variation of strain rate with vertical distance from the moving anvil is assumed, a strain-rate distribution as shown in Fig. 9 will result. However, Sn–Pb eutectic alloy is highly strain-rate sensitive [25] and therefore, the flow is easier at the lower strain rates. Then the lower portions, which experience slower strain rates, will undergo greater deformation and give rise to the observed results (see also Fig. 9).

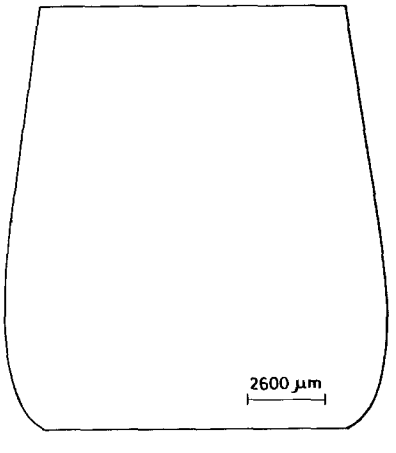

Figure 4 Shape changes in Plasticine compressed by (a) 10%, (b) 20%, (c) 30%, (d) 40%, and (e) 50%.

Similarly, the deformation behaviour of Plasticine, except when the height reduction was 20%, and the Sn–Pb eutectic alloy with a height-to-diameter ratio of 2.0, which was similar, can be understood following similar arguments. However, in those specimens a linear variation of strain rate existed only up to a certain depth (see Tables III and V). Later, the variation in strain rate became more rapid. Towards the bottom end, friction also appeared to be important. The net effect was that the compound curve consisted of a straight line (top) and a parabola. A possible strain-rate variation that can give rise to the observed strain distribution is given in Fig. 10.

After checking the reproducibility of the results three times, it has been concluded that following the compression of the Plasticine specimens by 20% the surface profile obtained was distinctly different (Fig. 3b): the compound curve obtained is made up of two parabolas, the top one descending to a distance of $H_f/3$. It is tempting to state that the compression specimen may be looked upon as a composite of two shorter specimens, each of which deforms to a parabola. This approach, however, overlooks the following aspects:

TABLE VA Prediction equations for Sn–Pb eutectic alloy of height-to-diameter ratio of 2.0 compressed, without a lubricant, by different amounts for a polynomial fit of degree three

$\left(\frac{H_0 - H_f}{H_0}\right) \times 100$ (%)	Prediction equation* (Measurements in mm)	Standard deviation (± mm)	Coefficient of variation (%)	True stress at the end of stroke (MN m^{-2})
20	$y = 0.0693 - 0.1767x + 0.1933x^2 - 0.0462x^3$	0.01	1.2	7
30	$y = 0.0226 + 0.0371x + 0.1185x^2 - 0.043x^3$	0.01	1.1	7

TABLE VB Prediction equation for Sn–Pb eutectic alloy of height-to-diameter ratio of 2.0 compressed, without a lubricant, by different amounts for a polynomial fit of degree four

$\left(\frac{H_0 - H_f}{H_0}\right) \times 100$ (%)	Prediction equation* (Measurements in mm)	Standard deviation (± mm)	Coefficient of variation (%)	True stress at the end of stroke (MN cm^{-2})
20	$y = 0.1372 - 0.4823x + 0.5826x^2 - 0.238x^3 + 0.0290x^4$	0.01	0.8	7
30	$y = 0.00775 + 0.2089x - 0.1248x^2 + 0.0819x^3 - 0.0213x^4$	< 0.01	0.3	7

TABLE VC Prediction equations for Sn–Pb eutectic alloy of height-to-diameter ratio of 2.0 compressed, without a lubricant, by different amounts for a fit obtained by dividing the compound curves into two parts

$\left(\frac{H_0 - H_f}{H_0}\right) \times 100$ (%)	Prediction equation (Measurements in mm)	Standard deviation (± mm)	Coefficient of variation (%)	True stress at the end of stroke (MN cm^{-2})
20	$y = 0.0190 + 0.0587x$	Nil	Nil	7
	$y = 0.0430 + 0.2332x - 0.1619x^2$	< 0.01	0.7	
30	$y = 0.13 + 0.10x$	Nil	Nil	7
	$y = 0.1519 + 0.2949x - 0.2617x^2$	< 0.01	0.9	

*The origin has been assumed to lie on the top surface of the specimen. (The original dimensions of the compression specimen have been magnified 20 times to obtain the prediction equations.) The ratio of the linear to the quadratic range is 1:1.

(a) no such observation could be made when the per cent compression was 10, 30, 40 or 50;

(b) the material has a high strain-rate sensitivity; and

(c) the top parabola terminates at a distance of $H_f/3$ and not $H_f/2$.

A possible strain-rate variation which can give rise to the present strain distribution is given in Fig. 11.

Surface shape changes during the upsetting of materials of high strain-rate sensitivity are not well understood. The results concerning the Sn–Pb

TABLE VI Mean and peak roughness values (see text) in case of commercial aluminium compressed, with and without a lubricant, by different amounts

$\left(\frac{H_0 - H_f}{H_0}\right) \times 100$ (%)	Condition	Surface Roughness		Diameter of compressed parallel face (mm)	Diameter of inner ring formed on parallel face (mm)
		R_a (μm)	R_t (μm)		
10	Unlubricated	0.02	0.16	10.5	10.1
20		0.02	0.40	11.4	10.1
30		0.30	1.80	12.0	10.1
40		0.30	2.60	13.0	10.1
50		0.45	3.00	14.4	10.1
10	Lubricated with	0.02	0.16	10.5	10.1
20	lithium-base grease	0.12	1.35	11.5	10.1
30		0.30	2.25	12.3	10.2
40		0.45	3.40	13.4	10.4
50		0.70	7.60	14.7	10.5

TABLE VII Mean and peak roughness values (see text) in the case of Sn–Pb eutectic alloy specimens compressed, with and without a lubricant, by different amounts

$\left(\frac{H_0 - H_f}{H_0}\right) \times 100$ (%)	Condition	Surface roughness		Diameter of compressed parallel face (mm)	Diameter of inner ring formed on parallel face (mm)
		R_a (μm)	R_t (μm)		
10	Unlubricated	0.04	0.26	10.5	10.1
20		0.20	2.70	11.4	10.1
30		0.25	3.20	12.0	10.1
40		0.30	3.60	13.0	10.1
50		0.40	3.30	14.4	10.1
10	Lubricated with	0.025	1.60	10.5	10.1
20	lithium-base grease	0.20	2.20	11.4	10.1
30		0.35	3.30	12.3	10.3
40		0.40	4.60	13.3	10.4
50		0.50	7.50	14.7	10.5

alloy specimens of height-to-diameter ratio 1.5 can be rationalized by suggesting that a linear variation in strain-rate (the simplest possibility) developed during upsetting. For the Plasticine specimens and the Sn–Pb alloy specimens of height-to-diameter ratio 2.0, whose response was similar, the observed strain distribution could be explained only in terms of more complicated variations in strain-rate. Future theoretical work should be directed towards quantifying the ideas concerning the combined effects of strain-rate sensitivity, friction and height-to-diameter ratio. Until this happens, empirical equations, like the ones developed in this paper, should be useful in predicting the surface contours developed during axi-symmetric upsetting, under different experimental conditions.

In this study the roughnesses of the flat faces of the cylindrical specimens prior to compression were measured. As all the specimens except those made of Plasticine (on which no roughness measurements were made) were fine-turned and their end faces polished down to 4/0 grade fineness of emery paper, it was assumed that their initial roughness was identical.

When considering the results it must also be noted that the maximum roughness value, R_t, is not reliable because even the presence of a single scratch can give rise to a high R_t value. So, greater emphasis was placed on the arithmetical mean roughness value, R_a.

For all of the specimens on which a roughness measurement was made, the diameter in contact with the platens had increased after a compression test, i.e., some of the material on the cylindrical sides had appeared at the material–die interface. This observation has been explained as follows: a "particle" of metal outside the friction-affected zone initially moves laterally until the downward movement of the tool either overtakes it or builds up sufficient stress to press it down.

Following relatively small deformation, the surface roughnesses of the lubricated specimens were comparable to or less than those observed in unlubricated specimens. However, after larger deformation their roughnesses were greater than those of the unlubricated specimens. While the former observation is only to be expected, the latter result can be traced to the greater flow of

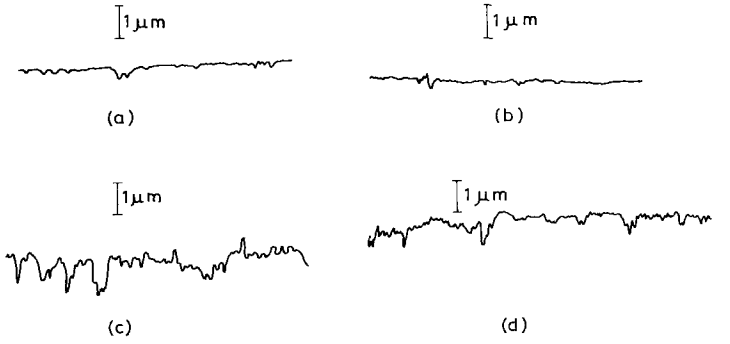

Figure 5 Surface roughness profiles in commercial aluminium compressed by (a) 10%, without a lubricant (b) 10%, with lithium-base grease as a lubricant (c) 20%, without a lubricant and (d) 20%, with lithium-base grease as a lubricant.

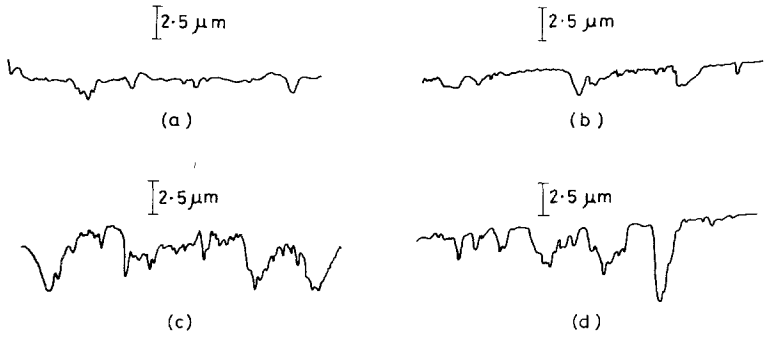

Figure 6 Surface roughness profiles in Sn–Pb eutectic alloy specimens compressed by (a) 20%, without a lubricant, (b) 20%, with lithium-base grease as a lubricant, (c) 40%, without a lubricant, and (d) 40%, with lithium-base grease as a lubricant.

surface metal in the lubricated specimens (Figs 7 and 8). (Evidently, a decrease in surface friction causes a greater flow of surface metal.)

A study of this kind may have the following advantages:

(a) There is a possibility that using the prediction equations generated for each type of flow, the initial specimen geometry for obtaining under free flow a given final shape can be determined. Also the machining required, after compression, at different places can be calculated *a priori*. Experiments have been planned in the second phase of this study to verify the above possibilities.

(b) The surface roughness after compression under different conditions can be determined. Of particular significance is the finding that after heavy reductions a lubricated specimen is likely to have a rougher surface compared with an unlubricated surface.

The question still remains as to whether the present results, obtained at a strain rate about 1000 times slower than industrial rates of forming, can be of use to industry. Firstly, it is noted that observations made at a similar strain-rate [26] for predicting strain–temperature combinations for controlled rolling, have subsequently been verified to be relevant in actual rolling experiments. (This is being reported elsewhere.) Secondly, in the next phase of this study experiments are being conducted in the strain-rate range of 0.5–10 sec^{-1}, using a hydraulic press and a friction-screw press. Those results, it is hoped, will show up the differences, if any, in surface contours arising out of a change in the strain-rate level.

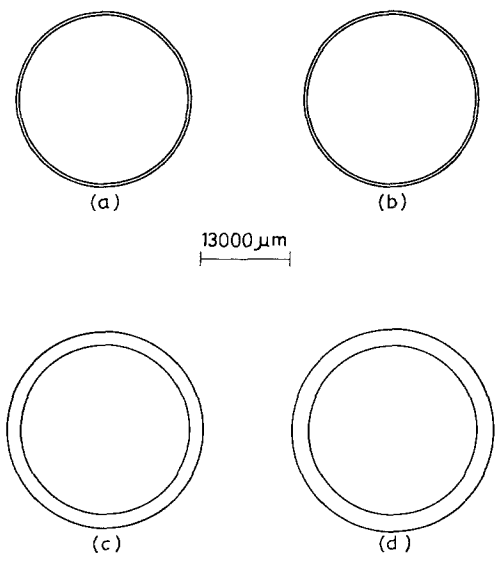

Figure 7 Outline of the compressed faces and the inner circles seen on the parallel faces of commercial aluminium compressed by (a) 10%, without a lubricant, (b) 10%, with lithium-base grease as a lubricant, (c) 20%, without a lubricant, and (d) 20%, with lithium-base grease as a lubricant.

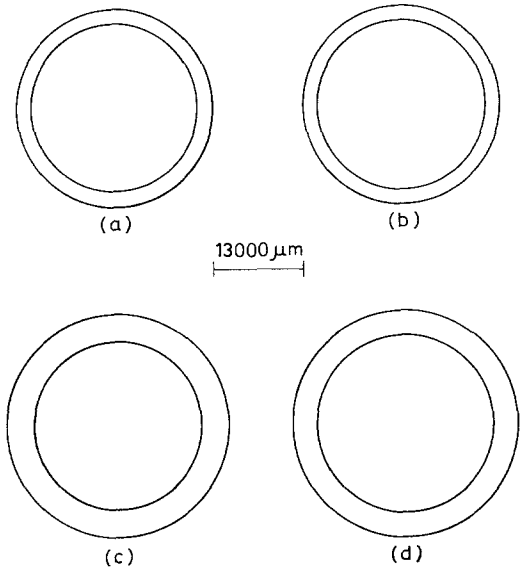

Figure 8 Outline of the compressed faces and the inner circles seen on parallel faces of Sn–Pb eutectic alloy compressed by (a) 20%, without a lubricant, (b) 20%, with lithium-base grease as a lubricant, (c) 40%, without a lubricant, and (d) 40%, with lithium-base grease as a lubricant.

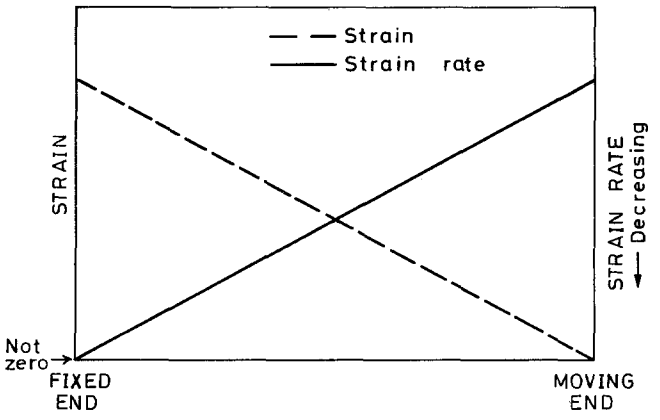

Figure 9 Schematic plot showing the variation of strain and strain-rate with vertical position in specimen for the Sn–Pb alloy specimens of H_0/D_0 ratio 1.5.

5. Conclusions

Based on axi-symmetric upsetting of aluminium specimens at a cold working temperature and Sn–Pb eutectic alloy and Plasticine specimens at hot working temperatures the following conclusions have been drawn:

(a) Compression of aluminium cylinders leads to barrelling, which can be represented by a parabola. Use of a lubricant reduces the flow stress and the extent of barrelling by about 5%.

(b) Compression of highly strain-rate sensitive Sn–Pb eutectic alloy specimens of height-to-diameter ratio of 1.5 causes a linear variation (with outward slope) of diameter from top to bottom.

(c) Compression of the Plasticine specimens and Sn–Pb eutectic alloy specimens having a height-to-diameter ratio of 2.0 gave rise to compound curved profiles which could be looked upon as a combination of either a straight line and a parabola or of two parabolas.

(d) The observed contours in aluminium are due to the presence of the friction-affected zones while in Sn–Pb eutectic alloy specimens of height-to-diameter ratio 1.5 the surface shape changes result from a linear decrease in strain-rate from the top to the bottom of specimens. The strain-rate variations required to explain the contours developed in Plasticine specimens and Sn–Pb alloy specimens of height-to-diameter ratio 2.0, on the other hand, are more complicated and cannot be predicted using the present knowledge concerning the upsetting of strain-rate sensitive materials.

Acknowledgements

The authors thank Professor V. Radhakrishnan for permitting the use of the profile projector and the Perth-o-meter. Professor S. L. Malhotra is thanked for his permission to use the Instron Universal Testing Machine. One of the authors (APS) thanks the Director, Indian Institute of Technology, Madras, for the provision of a research fellowship.

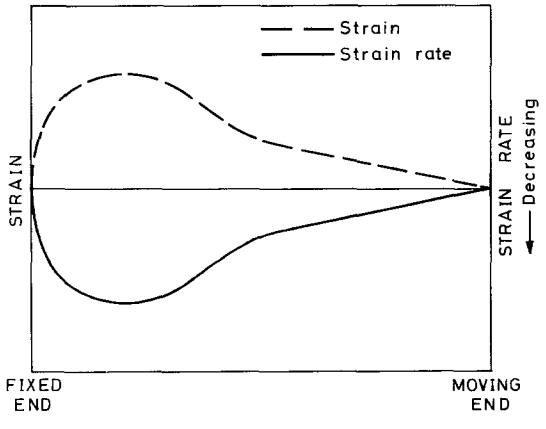

Figure 10 Schematic plot showing the variation of strain and strain-rate with vertical position in specimen for Plasticine (except when reduction was 20%) and Sn–Pb alloy ($H_0/D_0 = 2.0$) specimens.

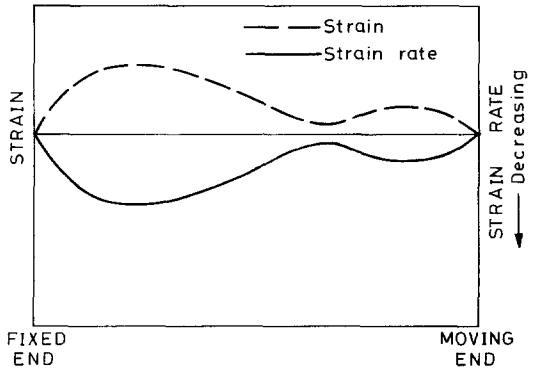

Figure 11 Schematic plot showing the variation of strain and strain-rate with vertical position in specimen for Plasticine compressed by 20%.

References

1. C. H. LEE and T. ALTAN, *J. Eng. Ind. Trans. ASME,* **94** (1972) 755.
2. J. M. ALEXANDER and R. C. BREWER, "Manufacturing Properties of Materials" (Von Nostrand, New York and London, 1971) p. 20.
3. W. JOHNSON and P. B. MELLOR, "Engineering Plasticity" (Van Nostrand, New York and London, 1973) pp. 350–367, 392, 393.
4. J. S. RINEHART and J. PEARSON, "Explosive Working of Metals" (Pergamon Press, Oxford and New York, 1963) pp. 130, 131, 179–181, 295–298.
5. E. WINKLER, *Canad. Met. Quart.* 7 (1968) 49.
6. K. M. KULKARNI and S. KALPAKJIAN, *J. Eng. Ind. Trans. ASME* **91** (1969) 743.
7. H. BUHLER and D. BUBBERT, *Industrie-Anzeiger* 88 (1966) 2175.
8. H. J. METZLER, *ibid.* **92** (1970) 1373.
9. T. C. HSU and A. J. YOUNG, *J. Strain Anal.* **2** (1967) 159.
10. P. F. THOMSON and J. S. HOGGART, *J. Inst. Met.* **96** (1968) 40.
11. L. H. BUTLER, *J. Inst. Petroleum* **40** (1954) 337.
12. P. W. WHITTON and H. FORD, *Proc. Inst. Mech. Eng.* **169** (1955) 123.
13. L. H. BUTLER, *Metallurgia* **55** (1957) 69.
14. *Idem, J. Inst. Met.* 88 (1959–60) 337.
15. *Idem, ibid.* 89 (1960–61) 116.
16. *Idem, Sheet Met. Ind.* **33** (1956) 647.
17. D. V. WILSON and G. W. ROWE, *J. Inst. Met.* **95** (1967) 25.
18. P. R. LANCASTER and G. W. ROWE, *Wear* **2** (1958–59) 428.
19. S. FUKUI, K. YOSHIDE, K. ABE and K. OZAKI, *Sheet Met. Ind.* **40** (1963) 439.
20. G. W. PEARSALL and W. A. BACKOFEN, *Trans. Amer. Soc. Mech. Eng.* **85** (1963) 68.
21. H. J. E. HAMMEL, *J. South African Inst. Min. and Met.* **72** (1972) 44.
22. B. AVITZUR, "Metal Forming: Processes and Analysis" (McGraw-Hill, New York, 1968) pp. 102–111.
23. G. KAMENSHCHIKOV, S. KOLTUN, V. NAUMOV and B. CHERNOBROVKIN, "Forging Practice" (Peace Publishers, Moscow) p. 163.
24. K. A. PADMANABHAN, Ph.D. thesis, University of Cambridge, 1971.
25. K. A. PADMANABHAN and G. J. DAVIES, "Superplasticity" (Springer Verlag, Berlin, Heidelberg and New York, 1980).
26. A. P. SINGH and K. A. PADMANABHAN, *Mater. Sci. Eng.* **51** (1981) 137.

Received 3 June
and accepted 28 July 1981